Accepted Manuscript

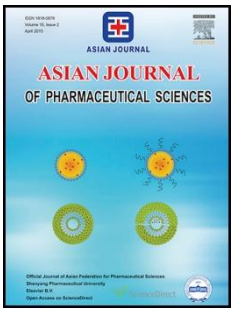

Title: **Exploring the potential of porous silicas as a carrier system for dissolution rate enhancement of artemether**.

Author: Jaywant N. Pawar, Harita R. Desai, Kailas K. Moravkar, Deepak Khanna, Purnima D. Amin

PII: S1818-0876(16)30039-3
DOI: http://dx.doi.org/doi: 10.1016/j.ajps.2016.06.002
Reference: AJPS 380

To appear in: *Asian Journal of Pharmaceutical Sciences*

Received date: 5-3-2016
Revised date: 10-5-2016
Accepted date: 3-6-2016

Please cite this article as: Jaywant N. Pawar, Harita R. Desai, Kailas K. Moravkar, Deepak Khanna, Purnima D. Amin, **Exploring the potential of porous silicas as a carrier system for dissolution rate enhancement of artemether**., *Asian Journal of Pharmaceutical Sciences* (2016), http://dx.doi.org/doi: 10.1016/j.ajps.2016.06.002.

TITLE:

Exploring the potential of porous silicas as a carrier system for dissolution rate enhancement of Artemether.

AUTHORS:

Jaywant N. Pawar[*1], Harita R. Desai[1], Kailas K. Moravkar[1], Deepak Khanna[2], Purnima D. Amin[1]

1. Department of Pharmaceutical Sciences and Technology, Institute of Chemical Technology (Elite Status), N. P. Marg, Matunga (E), Mumbai 400019, India.
2. Applied Technology, Inorganic Materials, Evonik Degussa India Pvt. Ltd., Krislon House, Sakivihar Road, Sakinaka, Andheri (East), Mumbai 400069, India

Corresponding author

Mr. Jaywant N. Pawar
Senior Research Fellow
Department of Pharmaceutical Sciences and Technology,
Institute of Chemical Technology Elite Status,
Matunga, Mumbai – 400019, India.
Tel.:+91 33612211; Fax: +91 33611020.
Email Id – jaywantpawar.ict@gmail.com

Abstract

Malaria is a parasitic and vector determined blood-conceived infectious disease transmitted through infected mosquitoes. Anti-malarial drug resistance is a major health problem, which hinders the control of malaria. Drug-resistant malaria when surveyed, the results demonstrated safe proclivity to nearby all anti-malarial regimes accessible except from

artemisinin and its derivatives. Artemether is a BCS class IV drug effective against acute and severe falciparum malaria hence; there is a strong need to improve its solubility. Silica is one of the most widely studied excipient. Silica can be used in solubility enhancement by preparing its solid solution/dispersion with the drug. The objective of this research was to improve dissolution rate of Artemether using non-precipitated porous silica (Aeroperl® 300 Pharma) and precipitated silica like (EXP.9555, EXP.9560, and EXP. 9565). Specific surface area calculated from BET method of porous silicas viz. APL 300 (A), Exp. 9555 (B), Exp. 9560 (C), Exp. 9565 (D). was found to be 294.13 m^2/g (A), 256.02 m^2/g (B), 213.62 m^2/g (C) and 207.22 m^2/g respectively.The drug release from the developed formulation was found to be significantly higher as compared to neat ARM. This improved solubility and release kinetics of ARM may be attributed to high surface area, improved wettability and decreased crystallinity. Solid-state characterization of the developed optimized formulation F3 was carried out with respect to FTIR chemical imaging, XRD, SEM, and DSC. All the porous silicas which we have explored in present context, showed a significant capability as a carrier for solubility enhancement of ARM.

Keywords: Artemether, solubility, solid dispersion, porous silica, Aeropearl® 300**.**

Abbreviations: Artemether [ARM], PS [porous silica], ARM:PS system [artemether : porous silica system]

1. Introduction

Drugs with poor aqueous solubility have low or erratic absorption and, subsequently poor bioavailability [1]. Some of the drugs that belong to class IV of the biopharmaceutical classification system are characterized by poor permeability and low aqueous solubility[2, 3]. Current statistics report that because of the low aqueous solubility, up to 40% of new chemical entities fail to reach market despite revealing potential pharmacodynamics activities.

Many potential compounds, often drop out on the way of pharmaceutical development because of their insufficient oral bioavailability. Consequently, lot of efforts have been made

to increase dissolution rate of such drugs. Different approaches to enhance the dissolution rate of poorly soluble drugs include, solid dispersions prepared by spray-drying [4-6], freeze-drying [7], mechanical milling [8, 9], hot melt extrusion [10, 11], supercritical fluid precipitation [12, 13], co-crystal formation [14], inclusion complexes using cyclodextrins[15], liquid antisolvent precipitation [16], loading onto porous carriers [17], amorphous solid dispersions by hot melt extrusion [18]. However, most of these technologies face demerits of scale up issue and economic challenge.

Malaria is a parasitic and vector determined blood-conceived infectious disease transmitted through infected mosquitoes. Anti-malarial drug resistance is a major health problem, which hinders the control of malaria. Drug-resistant malaria when surveyed, the results demonstrated safe proclivity to nearby all anti-malarial regimes accessible except from artemisinin and its derivatives. Artemisinin is an important type of antimalarial drugs, structurally characterised by incidence of a sesquiterpene lactone with a peroxide bridge [19, 20]. Different types of artemisinin derivatives has been synthesized viz. artemether, artesunate, arteether are currently in use [21].

Artemether [ARM] (chemical structure as shown in Fig. 1) is a potent antimalarial agent accessible for the treatment of severe multiresistant malaria and is included in WHO list of essential medicines. It is active against Plasmodium vivax as well as chloroquine-sensitive and chloroquine-resistant strains of Plasmodium falciparum. ARM, shows rapid onset of schizontocidal action and is metabolized in the liver to a demethylated derivative, dihydroartemisinin that is indicated in treatment of cerebral malaria. However, the therapeutic potential of ARM is significantly delayed due to its low oral bioavailability because of its poor aqueous solubility [22, 23].

Solvent evaporation method involves preparation of a solution containing both carrier material and drug, and the removal of the solvent resulting in the formation of the solid powder

mass. Preparation of SDs using solvent evaporation has been successfully explored for the dissolution rate enhancement of poorly water-soluble drugs [24-26]. In the present study, potential of various porous silica to improve the dissolution of ARM has been studied. Silica is one of the most widely studied excipient. It exists in amorphous to highly ordered crystalline states. Silica is generally regarded as safe [27]. The amorphous silica has lot of application in pharmaceutics and drug delivery such as glidant (flow promoter), carrier, thickener and viscosity modifier, adsorbent and preservative. Various reports are available in literature implementing its use in solubility enhancement by preparing its solid solution/dispersion with the drug. For example solid dispersion formulations using porous silicas [24,25] and bicalcutamide using Aeroperl® 300 (APL300) [30].

In this context, we have explored use of porous silicas like non-precipitated silica as APL 300 and precipitated porous silicas viz. EXP. 9555, EXP.9560, EXP.9565 as a carrier and adsorbent to formulate ARM:PS systems. All porous silicas had an inert amorphous material consisting of colloidal silicon dioxide with a significantly high pore volume and consistent spherical shape. Silica exists in amorphous to highly ordered crystalline states. It also has excellent flow and compressibility properties. Porous silicas in ARM:PS system can potentially resolve the formulation issues associated with solid dispersions. In addition, porous silicas are less likely to promote reversion of the amorphous drug to crystalline state on storage of solid dispersion due to its non-crystalline nature [30, 31]. Solid dispersion prepared using hydrophilic excipients often face softness and tackiness issues. To overcome such issues use of large amount of excipients is reported [32, 33]. The use of such excipients at higher amount often resulted into large tablet weights, which is not acceptable practically.

Hence, in this research work we have explored different types of porous silicas as a carrier system for the dissolution rate enhancement of poorly water-soluble drugs. ARM loading into porous silica by solvent evaporation method was explored at various ratios. Molecular state of drug in the prepared samples was evaluated using FTIR chemical imaging analysis, differential scanning calorimetry and powder X-ray diffractometry. Surface morphology study was carried out using scanning electron microscopy. The apparent solubility and dissolution behaviour of ARM:PS systems were evaluated further.

2. Materials and methods

2.1 Materials

Artemether was obtained as a generous gift from IPCA Pvt. Ltd. Mumbai, India. Aeroperl®300 pharma and other porous silicas viz. EXP. 9555, EXP.9560, EXP.9565 were obtained from Evonik industries, Germany. Hard gelatin capsules IP were obtained as a gift sample from ACG associated capsules Pvt. Ltd. India. All other chemicals and solvents used were of analytical grade and were procured from Merck India Ltd. All the materials were used as received.

2.2 Methods

2.1 Preparation of ARM-PS systems

ARM:PS systems were prepared by solvent evaporation technique. ARM (1 gm) was dissolved in 5 ml of acetone under stirring to form a transparent solution. After complete homogenization ratios as 1:1, 1:2 and 1:3 of respective porous silicas were added in solvent system as shown in Table 1. The solution was covered with an Aluminum foil and the solvent from the clear solution was allowed to be evaporated by piercing 5-6 fine holes in the foil. The entire process was carried out at room temperature with constant stirring. The process was continued till a solid fine product was obtained. The product was dried in vacuum oven at 40°C for 5 minute cycles until constant weight has attained. The obtained product was

pulverized and passed through size 60# mesh sieve. Obtained product was kept in desiccator for further evaluation for various parameters.

2.3 Saturation solubility study

The equilibrium solubility study of neat ARM and prepared ARM:PS systems were carried out in 10 mL of distilled water containing 1 % SLS and phosphate buffer of pH 7.2 containing 1 % SLS evaluated for maximum solubility of ARM and ARM:PS system in respective dissolution media after 72 hrs. By adding an excess amount of neat ARM and ARM:PS system (F1 – F12). The samples then sonicated for 15min at room temperature. Thereafter, the test tubes (n=3) were shaken for 72 hrs at 37 ± 0.5°C at a speed of 75 rpm on an orbital shaking thermo stable incubator (Boekel Scientific, Germany). The samples were centrifuged at 10000 rpm for 15 min and filtered through 0.45 µm millipore membrane filter. The first 1 mL of the filtrate was discarded. Samples were then suitably diluted with respective dissolution medium and analyzed at 211 nm on UV- spectrophotometer (UV- 1601 PC, Shimadzu, Japan).

2.4 *In vitro* release study

The *in vitro* drug dissolution properties of ARM:PS systems were examined according to the USP basket method using dissolution apparatus (Electrolab Pvt. Ltd. India) at 37 ± 0.5°C. Powder samples equivalent to 40 mg of ARM:PS system (F1 – F12) were filled in hard gelatin capsules were added to dissolution media containing 1000mL phosphate buffer of pH 7.2 with 1% SLS (sodium lauryl sulphate) at a temperature of 37 ± 0.2° C. The solution was stirred with a rotating basket at 100 rpm. Aliquots of 5.0 mL were withdrawn from each vessel at predetermined time intervals [10, 20, 30, 40, 50, 60 and 120 min], filtered over a cellulose acetate filter of 0.45 μ. At each time point, the same volume of fresh preheated

dissolution medium was replaced. The ARM concentration in each sampled aliquot was determined using an ultraviolet visible spectrophotometer at 211 nm (UV-1601PC, Shimadzu, Japan).

2.5 Differential scanning calorimetry

DSC analysis was performed using Pyris-6 DSC Perkin Elmer (USA). Approximately 4 mg of sample was placed in aluminium pan and crimped using a press. An empty aluminium pan was used as a reference pan. Experiment was carried out in nitrogen atmosphere 17 mL/min of nitrogen flow at a heating rate of 10°C/minute from 30°C to 300°C to obtain the endothermic peaks.

2.6 X-ray diffraction analysis

The X-ray diffraction studies of pure ARM, APL 300, Exp. 9555, Exp. 9560 and Exp. 9565 and all ARM:PS system (F1 – F12) with porous silicas were recorded using ADVANCE D8 system with CuKα radiation (Bruker, USA). XRD studies were carried out to determine whether the sample is in crystalline, paracrystalline or amorphous state. The voltage of 40 kV with current 20 mA was set. The recording spectral range was set at 10° to 50° two theta values using the Cu-target X-ray tube and Xe-filled detector. The step scan mode was performed with a step size of 0.02° at a rate of 2° min-1. The samples were placed in a zero background sample holder and incorporated on a spinner stage. Soller slits (0.04 rad) were used in the incident and diffracted beam path.

2.7 Scanning electron microscopy

To learn the particulate morphologies of ARM powder and ARM:PS system (F3, F6, F9 and F12) were examined using XL 30 Model JEOL 6800 scanning electron microscope (Japan), during analysis double-sided carbon tape was affixed on aluminium stubs over which powder sample of ARM and ARM-PS were sprinkled. The radiation of platinum plasma beam using JFC-1600 auto fine coater was targeted on aluminium stubs for its coating to make layer of 2

nm thickness above the sprinkled powder for 30 min. Then, those samples were observed for morphological characterization using a gaseous secondary electron detector (working pressure: 0.8 Torr, acceleration voltage: 10-30.00 kV).

2.8 Powder flow properties

The parameters governing flow properties of ARM-PS systems were calculated using USP (2007) methods. The bulk volume of the undisturbed powder when filled in a 50 ml graduated cylinder was measured and bulk density [34] was calculated using Venkel tapped density apparatus (Japan) after mechanical 500 taps, which provided tapped density (TD). Hausner's ratio and compressibility index were calculated using equations I and II [35].

$$\text{Hausner's ratio} = TD/BD \quad (1)$$

$$\text{Compressibility index} = 100\,(TD-BD)\,/\,TD \quad (2)$$

2.9 Moisture content of ARM-PS carrier systems

Approximately 1-2 grams of ARM:PS system (F1 – F12) were evaluated for moisture content using the Citizen digital moisture analyzer balance (India) and the moisture content was determined in percentage.

2.10 Encapsulation efficiency study

An amount of ARM:PS system (F1 – F12) samples containing about 40mg of ARM was weighed and dissolved in sufficient methanol to produce 100ml. The resulting solution was filtered using a sintered glass crucible, discarding the first 10mls. 2ml of the resulting solution was pipetted into a quick-fit test tube and 2ml of concentrated HCl added. The test tube was stoppered and allowed to stand in a water bath set to 30 ˚C (or room temp.) for 25 minutes. The resulting solution was diluted with sufficient methanol to 50ml. The absorbance reading at a wavelength maximum of 211 nm was taken against a blank solution made up of

2ml of HCl made up to 50ml with methanol. The encapsulation efficiency of ARM in the prepared ARM:PS system were calculated from calibration curve.

2.11 Specific Surface Area and Pore Size Distribution

The surface area of developed porous starch was deter-mined using nitrogen sorption isotherms through Brumauer–Emmett – Teller (BET) protocol. Nitrogen sorption studies were done using ASA P2020 (Micromeritics , USA) . Before initiation of the study, the powder sample was stored in sample bulb and then subjected to 40°C under vacuum of 0.1 mPa overnight to facilitate removal of moisture from the sample. The nitrogen sorption data were generated through a relative pressure (p/ p0) range of 0.0 to 1.0.

3. Results and discussion

3.1 Saturation solubility study

The saturation solubility study of the developed ARM:PS system showed increase in drug solubility with increase in ratios of respective porous silica. The solubility of neat ARM shows very least solubility value 0.0180 µg/mL in distilled water containing 1% SLS. Fig. 2 shows the solubility data of ARM:PS system of ARM with different porous silicas showed an improved solubility profile compared to neat ARM in both dissolution media. In F3 formulation batch of ARM with APL 300, EXP. 9555, EXP. 9560 and EXP. 9565 enhanced the solubility up to an extent F3 = 22.03 µg/mL, F6 = 32.04 µg/mL, F9 = 31.08 and F12 = 29.08 µg/mL respectively in dissolution medium of distilled water containing 1% SLS.

The saturation solubility of ARM:PS systems found higher in medium 2 containing phosphate buffer (pH 7.2) containing 1 % SLS with solubility values of ARM:PS systems as F3 = 138.94 µg/mL, F6 = 137.84 µg/mL, F9 = 125.69 and F12 = 119.65 µg/mL respectively. A linear relationship with respect to increase in solubility of ARM to respective increased

ratios of porous silica's to drug were observed shown in Fig. 2. The solubility data of ARM:PS systems with different porous silicas showed an improved solubility profile compared to neat ARM. As per the Noyes-Whitney equation [36, 37], saturation solubility and dissolution rate of a drug can be increased by increase in surface area of particles. In case of ARM:PS system the drug is adsorbed in the pores of, the porous silica resulted in particle size reduction of drug particles. The saturation solubility results are in good agreement with Noyes-Whitney equation [38]. The increase in solubility of system could be due to improved wettability of ARM. Adsorption of the drug particles in the pores of porous silica resulted in decrease in particle size of drug particles resulting into formation of amorphous ARM.

3.2 Differential scanning calorimetry studies

Thermal behaviour of neat ARM, APL 300, EXP. 9555, EXP. 9560, EXP. 9560, EXP. 9565, and ARM:PS systems F3, F6, F9, and F12 are shown in Fig. 3. The pure ARM shows a sharp endothermic peak at 86.64 ^{o}C, followed by exothermic peak at 172.21 ^{o}C with enthalpy change of 56.68 J/g, whereas APL 300 and other porous silica did not show a melting endotherm because of its amorphous nature. The thermogram of ARM:PS systems showed slight decrease in ΔH and peak height, in accordance with XRD diffractograms. In case of DSC analysis characteristic endothermic peak of ARM was shifted towards higher temperature with reduced intensity in ARM:PS system. The F3, F6 and F12 showed very small endothermic peak at a lower temperature compared to neat ARM indicating some crystallinity, that may be due to addition of excess amount of ARM in solvent evaporation process. The heat of fusion of neat ARM was higher compared to that of ARM:PS system. The heat of fusion decreased with increase in carrier ratio. The DSC thermograms indicated that the crystalline nature of ARM was diminished in ARM:PS system with increase in ratio of respective silicas. This could be attributed to higher APL 300 and other porous silica

concentration and uniform distribution of ARM in the porous silica, resulting in complete miscibility of drug in carrier system.

3.4 X-ray diffraction studies

X-ray diffraction studies were performed to elucidate the physical state of the pure ARM in the ARM:PS system. The X-ray diffarctograms of ARM, APL 300, F1, F2 and F3, Exp. 9555, F4, F5 and F6, Exp. 9560, F7, F8, and F9 and Exp. 9565, F10, F11, and F12 are shown in Fig. 4a, 4b, 4c and 4d respectively which illustrates the changes in drug crystallinity upon increasing ratios of respective porous silica. The X-ray diffarctograms of ARM show numerous distinct peaks at two-theta values of 7.29°, 10.04°, 18.04°, 19.68° and 22.1° indicating the crystalline nature of drug, results are in resemblance with previous literature [39, 40]. All porous silica are amorphous and did not produce any peaks. The high intensity signal of ARM drug at two-theta value of 10.04° was found to be significantly reduced in the XRD of F3, F2 & F1. Formulation systems F2 & F1 shows intense peak compared to F3 due to presence of ARM in more amount. X-ray diffraction studies were performed to study physical nature of ARM loaded with respective silicas. In case of, F5 & F6 does not shows any intense peak indicating complete amorphous state of formulation system nevertheless F4 shows some intense peak indicating partial amorphization. The formulation systems F7 to F9 and F10 to F12 loaded with ARM shows high intensity signal of ARM at two-theta value of 10.04° indicating partial adsorption of drug into porous silica. A broadened peak of all ARM loaded silicas at two-theta value of 22.10° could be contributed to the lowering of crystallite size of drug thus indicating partial amorphousness due to effect of drug loading on silica.

3.5 Scanning electron microscopy studies:

SEM was used to study to determine the surface morphologies of pure ARM, APL 300 and ARM:PS systems are shown in Fig. 5, from the SEM micrographs of pure ARM

revealed large crystalline particles with cubic shape blocks, comparatively larger than ARM:PS systems. The ARM:PS systems were found to be without sharp edges. The solid dispersion particles had a reduced geometric diameter at a range of several micrometres compared to pure ARM as shown in Fig-5 A, B, C, D and E. SEM study revelead that eextensive deposition of the ARM drug was observed on APL 300 as compared to EXP.9555, EXP. 9560 and EXP.9565 porous silica. This may be contributed to large surface area imparted by the porous nature of silica. The ARM:PS systems appeared to be agglomerated with smooth surface owing to presence of porous silica. The ARM:PS systems showed more homogeneity with porous silica.

3.6 In vitro dissolution rate studies of ARM:PS systems

The in-vitro dissolution profiles of pure ARM and ARM:PS system prepared by solvent evaporation method are represented in Fig. 6. The aqueous solubility of ARM is 0.019 µg/mL that can be considered as a practically insoluble drug in water. All solid dispersion systems displayed higher solubility of ARM than pure drug. Enhancement in dissolution rate of ARM:PS systems was observed in following order: APL 300 > EXP. 9555 > EXP. 9560 > EXP. 9565 with percentage dissolution found (F3= 68.9%), (F6= 63.77%), (F9= 60.04%), and (F12= 59.64%) respectively at end of T_{90} minutes compared with neat ARM (28.16 %).

The dissolution rate of ARM:PS systems has improved largely than neat ARM, with increase in amount of respective porous silica. The dissolution rate enhancement of ARM from drug-carrier systems was due to conversion of drug to amorphous state and solubilization effect of porous silica as a carrier resulting in enhanced wettability and an increased effective surface area of ARM. The enhancement in solubility is the result of disordered structure of amorphous solid that offers a lower thermodynamic barrier to dissolution and formation dispersion where the drug is adsorbed inside pores of porous

294 silicas. An amorphous formulation system will dissolve at a faster rate because of its
295 higher internal energy and superior molecular motion [41]. The porous silica favors to
296 insoluble ARM gets out in open dissolution medium in the form of very fine particulate
297 system for instant dissolution.

298 The results are in good agreement with that obtained from DSC and XRD
299 measurement that indicates drug incorporated in porous structure of silica was in amorphous
300 form. Dissolution efficiency (DE) is the area under the dissolution curve between time point's
301 t_1 and t_2 expressed as a percentage of curve at maximum dissolution, y100, over same time
302 period and is expressed by the following expression:

$$\text{Dissolution efficiency} = \frac{\int_{t1}^{t2} y.\,dt}{y100\ (t2 - t1)} \times 100$$

303 DE values indicates the real time dissolution rate of drug dissolved in dissolution medium.
304 DE values of F3, F6, F9 and F12 were found to be 75.58, 72.34, 71.9 and 73.12 respectively.
305 DE values gives us a superior illustrative information with reference to in vivo performance.

306 3.7 Flow properties measurement:

307 Powder flow and compaction behaviour play an important role in manufacturing,
308 processing and packaging techniques. ARM:PS systems were evaluated for powder flow
309 properties and values were found to be within the prescribed limits of all formulations as
310 shown in table 2. All formulations exhibited good flow property as expressed in term of
311 micrometric parameters as per USP guidelines and found within limit.

312 3.8 Moisture content of ARM-PS carrier systems

Approximately 1.5-2 grams of ARM:PS systems were loaded on pan on Citizen digital moisture analyzer balance, (India) and moisture content was determined in percentage. The moisture content values are as shown in table 3. The moisture content values of all the developed formulation systems found within USP limits.

3.9 Content uniformity of ARM-PS carrier systems

The content uniformity of ARM in the ARM: PS systems found uniformly distributed. All the % content values were found within range of (97-102%) as per international pharmacopoeia respective values of ARM:PS systems are shown in table 4. The content of ARM was calculated from the calibration curve equation (y = 0.303x + 0.0148). Therefore, x obtained from standard curve equation will correspond to: X*100/8= **X*12.5**. The % assay of ARM in the ARM: PS systems found uniformly distributed. The content uniformity was found within range of (97-102%) as per international pharmacopoeia.

3.10 Specific Surface Area and Pore Size Distribution

The nitrogen adsorption and desorption behaviour of all the porous silica samples has been shown in (Fig.7) APL 300 (A), Exp. 9555 (B), Exp. 9560 (C), Exp. 9565 (D). Specific surface area calculated from BET method was found to be 294.13 m^2/g (A), 256.02 m^2/g (B), 213.62 m^2/g (C) and 207.22 m^2/g respectively. All the results showed typeIV isotherm displaying a monolayer adsorption followed by multilayer adsorption of nitrogen on respective porous silicas. Nitrogen condensation step resulted in two hysteresis loops. The curve also showed nitrogen condensation step which is distinct feature of porous materailas [30]. The APL 300 showed highest specific surface area as it is made by non-precipitataion method, neverthless the other silicas made by precipitataion method. As APL 300 is having highest porous surface area showed highest solubility and dissolution rate compared to other porous silicas.

4. Conclusion

In the present study, dissolution rate enhancement potential of porous silica for ARM is successfully demonstrated. The results from FTIR chemical imaging, SEM, XRD and DSC analysis showed that ARM in amorphous form could be incorporated into porous silica by solvent evaporation method. The improved dissolution rate of ARM:PS systems is because of amorphous nature of ARM and better wetting properties induced by porous silica. This technique can effectively be extrapolated to number of other poorly water-soluble drugs in a cost effective way for preparation of immediate release formulations.

Acknowledgments

Authors would like to thank University grants commission, India for their financial support. Authors are grateful to Evonik Industries for providing gift samples of silicas viz. Aeroperl® 300 Pharma and Exp. 9555, Exp. 9560 and Exp. 9565.

Ethical issues

Author declares no ethical issues.

Competing interests

There is no known conflict of interest.

REFERENCES

[1]. Friesen DT, Shanker R, Crew M, et al. Hydroxypropyl methylcellulose acetate succinate-based spray-dried dispersions: an overview. Molecular pharmaceutics. 2008;5(6):1003-19.
[2]. Al-Hamidi H, Edwards AA, Mohammad MA et al. To enhance dissolution rate of poorly water-soluble drugs: glucosamine hydrochloride as a potential carrier in solid dispersion formulations. Colloids and Surfaces B: Biointerfaces. 2010;76(1):170-8.
[3]. Bikiaris DN. Solid dispersions, part I: recent evolutions and future opportunities in manufacturing methods for dissolution rate enhancement of poorly water-soluble drugs. Expert opinion on drug delivery. 2011;8(11):1501-19.

[4]. Paradkar A, Ambike AA, Jadhav BK, et al. Characterization of curcumin–PVP solid dispersion obtained by spray drying. International journal of pharmaceutics. 2004;271(1):281-6.
[5]. Gu B, Linehan B, Tseng Y-C. Optimization of the Büchi B-90 spray drying process using central composite design for preparation of solid dispersions. International journal of pharmaceutics. 2015;491(1):208-17.
[6]. Pawar JN, Shete RT, Gangurde AB et al. Development of amorphous dispersions of artemether with hydrophilic polymers via spray drying: Physicochemical and in silico studies. Asian Journal of Pharmaceutical Sciences. 2015.
[7]. Ansari MT, Hussain A, Nadeem S et al. Preparation and Characterization of Solid Dispersions of Artemether by Freeze-Dried Method. BioMed Research International. 2015;2015.
[8]. Branham ML, Moyo T, Govender T. Preparation and solid-state characterization of ball milled saquinavir mesylate for solubility enhancement. European Journal of Pharmaceutics and Biopharmaceutics. 2012;80(1):194-202.
[9]. Zhong L, Zhu X, Yu B, et al. Influence of alkalizers on dissolution properties of telmisartan in solid dispersions prepared by cogrinding. Drug development and industrial pharmacy. 2014;40(12):1660-9.
[10]. Crowley K, Gryczke A. Hot Melt Extrusion of Amorphous Solid Dispersions. Pharmaceutical Sciences Encyclopedia. 2015.
[11]. Alshahrani SM, Lu W, Park J-B, et al. Stability-enhanced Hot-melt Extruded Amorphous Solid Dispersions via Combinations of Soluplus® and HPMCAS-HF. AAPS PharmSciTech. 2015:1-11.
[12]. Sheth P, Sandhu H. Amorphous Solid Dispersion Using Supercritical Fluid Technology. Amorphous Solid Dispersions: Springer; 2014. p. 579-91.
[13]. Kim M-s, Kim J-s, Park HJ, et al. Enhanced bioavailability of sirolimus via preparation of solid dispersion nanoparticles using a supercritical antisolvent process. International journal of nanomedicine. 2011;6:2997.
[14]. Elder DP, Holm R, de Diego HL. Use of pharmaceutical salts and cocrystals to address the issue of poor solubility. International journal of pharmaceutics. 2013;453(1):88-100.
[15]. Taupitz T, Dressman JB, Buchanan CM, et al. Cyclodextrin-water soluble polymer ternary complexes enhance the solubility and dissolution behaviour of poorly soluble drugs. Case example: itraconazole. European Journal of Pharmaceutics and Biopharmaceutics. 2013;83(3):378-87.
[16]. Meer T, Sawant K, Amin P. Liquid antisolvent precipitation process for solubility modulation of bicalutamide. Acta Pharmaceutica. 2011;61(4):435-45.
[17]. Meer TA, Moravkar K, Pawar J, et al. Crosslinked Porous Starch Particles–a Promising Carrier. Polim Med. 2015;45(1):00-.
[18]. Pawar J, Tayade A, Gangurde A, et al. Solubility and dissolution enhancement of efavirenz hot melt extruded amorphous solid dispersions using combination of polymeric blends: A QbD approach. European Journal of Pharmaceutical Sciences. 2016;88:37-49.
[19]. Yang B, Lin J, Chen Y, et al. Artemether/hydroxypropyl-β-cyclodextrin host–guest system: Characterization, phase-solubility and inclusion mode. Bioorganic & medicinal chemistry. 2009;17(17):6311-7.
[20]. Meshnick SR. Artemisinin and its derivatives. Antimalarial Chemotherapy: Springer; 2001. p. 191-201.
[21]. Beteck RM, Smit FJ, Haynes RK, et al. Recent progress in the development of anti-malarial quinolones. Malaria journal. 2014;13(1):339.

[22]. Shah PP, Mashru RC. Development and evaluation of artemether taste masked rapid disintegrating tablets with improved dissolution using solid dispersion technique. AAPS PharmSciTech. 2008;9(2):494-500.
[23]. Amin PD. Artemether-soluplus hot-melt extrudate solid dispersion systems for solubility and dissolution rate enhancement with amorphous state characteristics. Journal of Pharmaceutics. 2013;2013.
[24]. Sethia S, Squillante E. Solid dispersion of carbamazepine in PVP K30 by conventional solvent evaporation and supercritical methods. International Journal of Pharmaceutics. 2004;272(1):1-10.
[25]. Ramesh K, Khadgapathi P, Bhikshapathi D, et al. Development, Characterization and in vivo evaluation of Tovaptan solid dispersions via solvent evaporation technique. International Journal of Drug Delivery. 2015;7(1):32-43.
[26]. Frizon F, de Oliveira Eloy J, Donaduzzi CM, et al. Dissolution rate enhancement of loratadine in polyvinylpyrrolidone K-30 solid dispersions by solvent methods. Powder Technology. 2013;235:532-9.
[27]. Lauer ME, Siam M, Tardio J, et al. Rapid assessment of homogeneity and stability of amorphous solid dispersions by atomic force microscopy—from bench to batch. Pharmaceutical research. 2013;30(8):2010-22.
[28]. Planinšek O, Kovačič B, Vrečer F. Carvedilol dissolution improvement by preparation of solid dispersions with porous silica. International journal of pharmaceutics. 2011;406(1):41-8.
[29]. Yan Hm, Sun E, Cui L, et al. Improvement in oral bioavailability and dissolution of tanshinone IIA by preparation of solid dispersions with porous silica. Journal of Pharmacy and Pharmacology. 2015.
[30]. Meer T, Fule R, Khanna D, et al. Solubility modulation of bicalutamide using porous silica. Journal of Pharmaceutical Investigation. 2013;43(4):279-85.
[31]. Singh D, Pathak K. Hydrogen bond replacement—Unearthing a novel molecular mechanism of surface solid dispersion for enhanced solubility of a drug for veterinary use. International journal of pharmaceutics. 2013;441(1):99-110.
[32]. Owusu-Ababio G, Ebube NK, Reams R, et al. Comparative dissolution studies for mefenamic acid-polyethylene glycol solid dispersion systems and tablets. Pharmaceutical development and technology. 1998;3(3):405-12.
[33]. Kubbinga M, Moghani L, Langguth P. Novel insights into excipient effects on the biopharmaceutics of APIs from different BCS classes: Lactose in solid oral dosage forms. European Journal of Pharmaceutical Sciences. 2014;61:27-31.
[34]. Feng X, Vo A, Patil H, et al. The effects of polymer carrier, hot melt extrusion process and downstream processing parameters on the moisture sorption properties of amorphous solid dispersions. Journal of Pharmacy and Pharmacology. 2015.
[35]. Gangurde AB, Fule RA, Pawar JN, et al.. Microencapsulation using aqueous dispersion of lipid matrix by fluidized bed processing technique for stabilization of choline salt. Journal of Pharmaceutical Investigation. 2015;45(2):209-21.
[36]. Humphreys DD, Friesner RA, Berne BJ. A multiple-time-step molecular dynamics algorithm for macromolecules. The Journal of Physical Chemistry. 1994;98(27):6885-92.
[37]. Müller R, Jacobs C, Kayser O. Nanosuspensions as particulate drug formulations in therapy: rationale for development and what we can expect for the future. Advanced drug delivery reviews. 2001;47(1):3-19.
[38]. Sahoo NG, Abbas A, Li CM. Micro/nanoparticle design and fabrication for pharmaceutical drug preparation and delivery applications. Current Drug Therapy. 2008;3(2):78-97.

[39]. Irene B, Veronica A, Laura A, Cosimo C. A hyperbranched polyester as antinucleating agent for Artemisinin in electrospun nanofibers. European Polymer Journal. 2014;60:145-52.
[40]. Mistry AK, Nagda CD, Nagda DC, Dixit BC, Dixit RB. Formulation and in vitro evaluation of ofloxacin tablets using natural gums as binders. Scientia pharmaceutica. 2014;82(2):441.
[41]. Subramaniam B, Rajewski RA, Snavely K. Pharmaceutical processing with supercritical carbon dioxide. Journal of pharmaceutical sciences. 1997;86(8):885-90.

Fig 1. Chemical structure of ARM

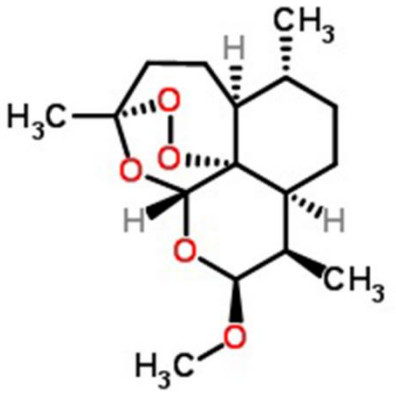

472 **Fig. 2.** Solubility of ARM and SDs **[**Medium 1: Distilled water containing 1 % SLS

473 Medium 2: Phosphate buffer pH 7.2 containing 1 % SLS**]**

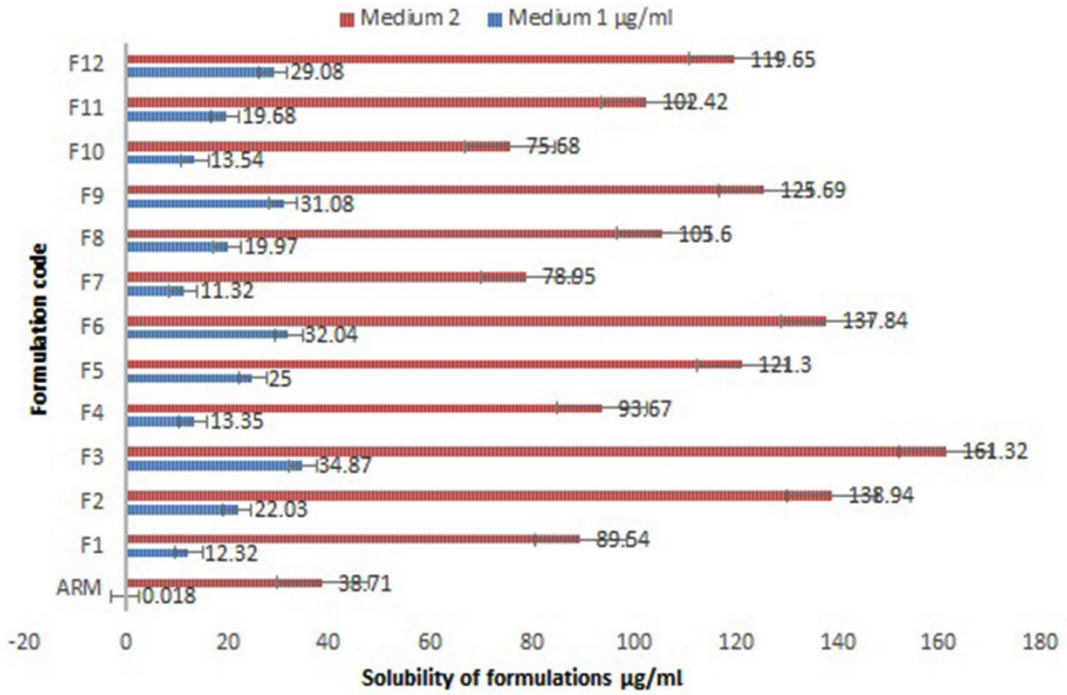

474

475

476

Fig. 3 DSC thermograms of Artemether (a), APL 300 (b), Exp. 9555 (c), Exp. 9560 (d), Exp. 9565 (e), F3 (f), F6 (g), F9 (h), F12 (i).

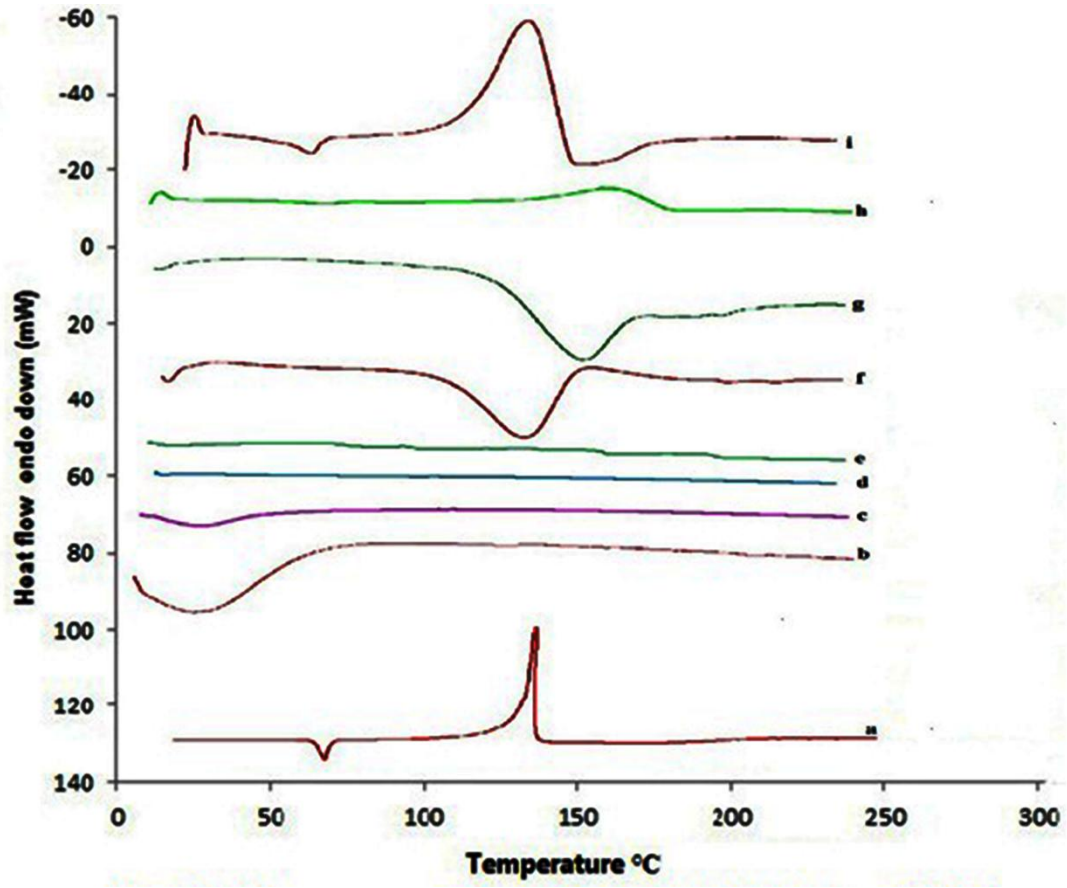

Fig. 4a – PXRD patterns of pure ARM and ARM loaded with APL300

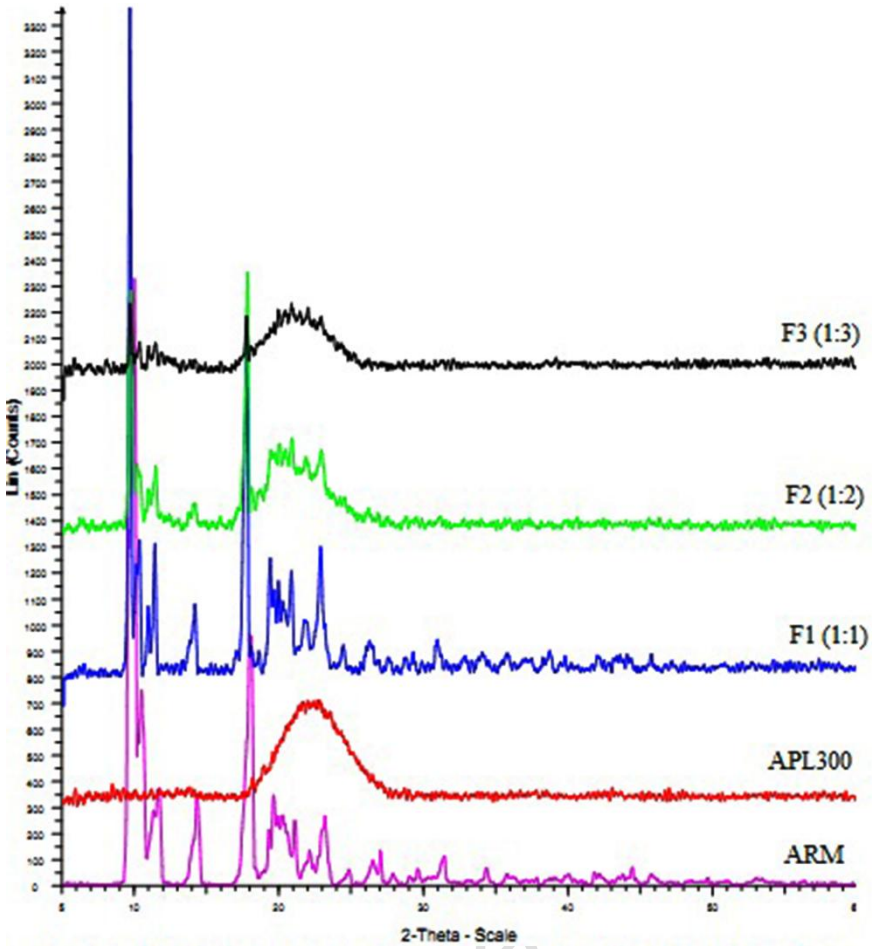

Fig. 4b – PXRD patterns of pure ARM and ARM loaded with EXP. 9555

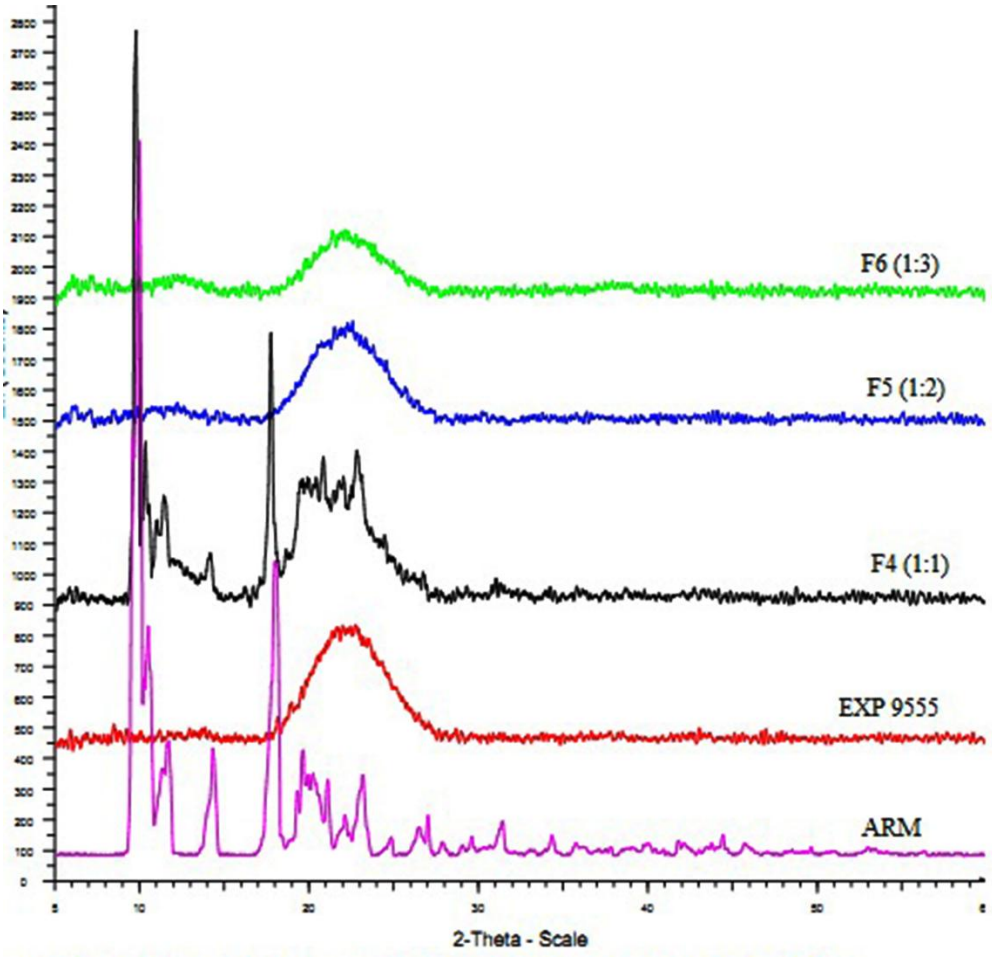

507 **Fig. 4c –** PXRD patterns of pure ARM and ARM loaded with EXP. 9560

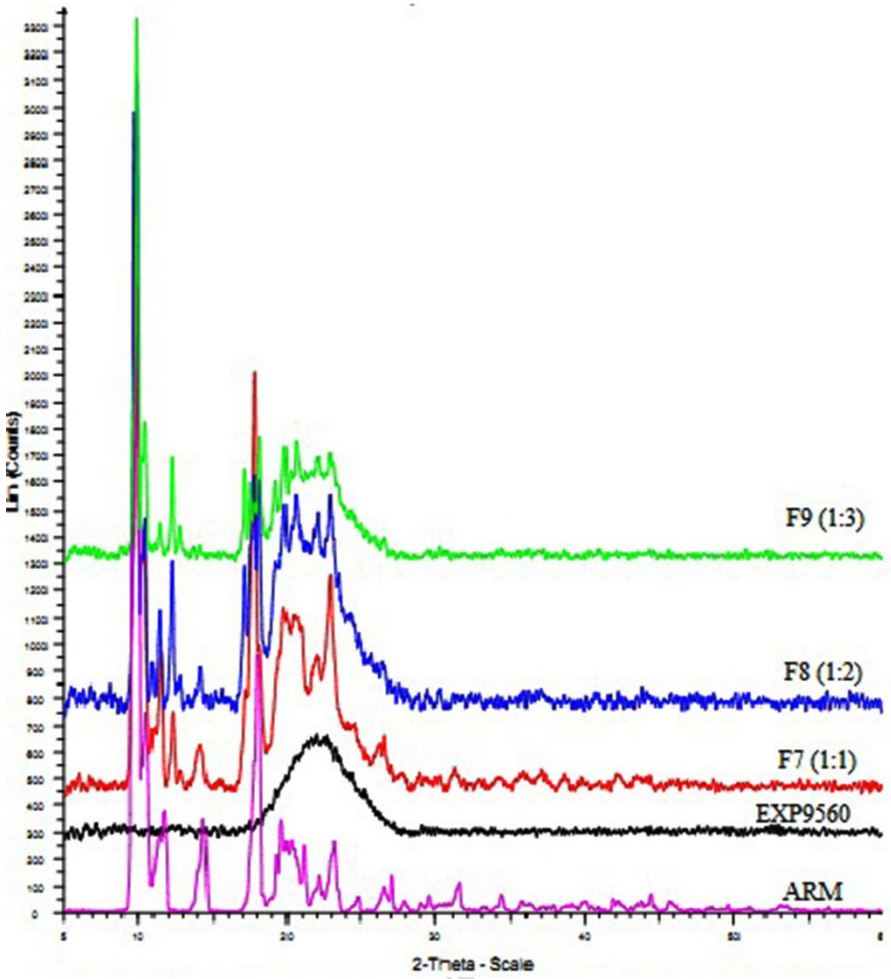

508

509

510

511

512

513

514

515

516 **Fig. 4d –** PXRD patterns of pure ARM and ARM loaded with EXP. 9565

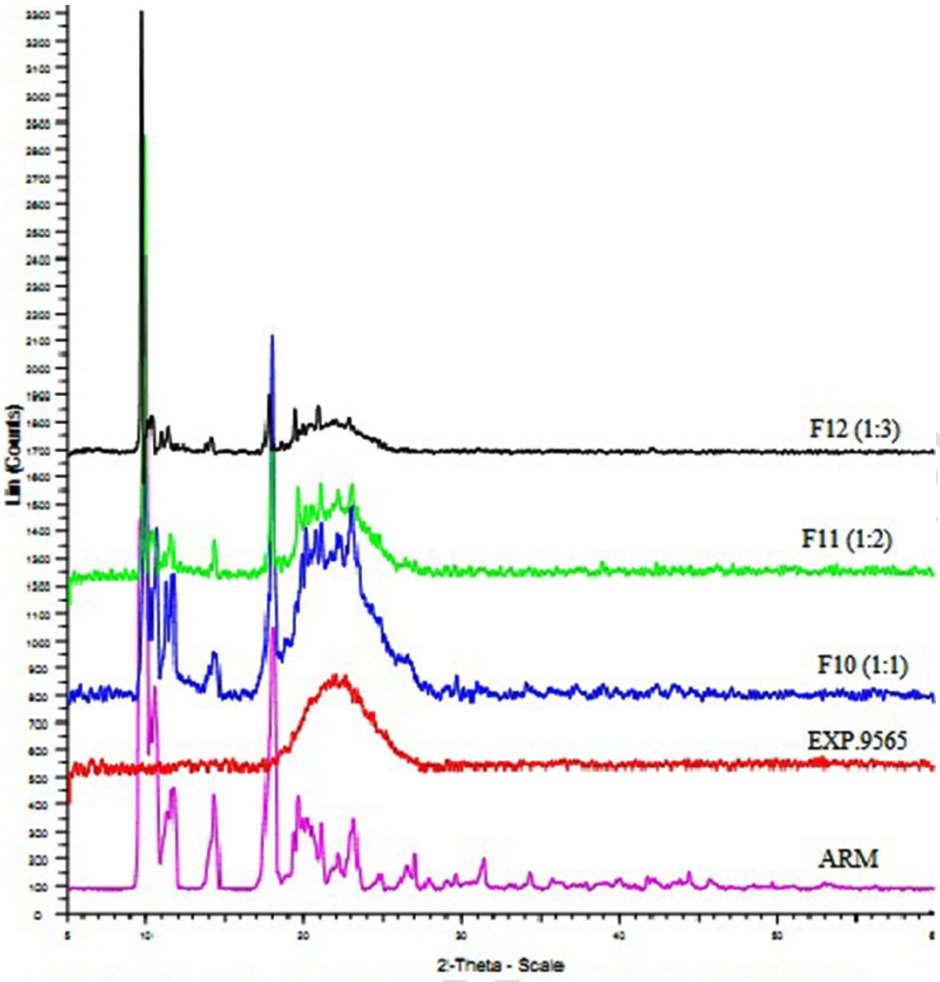

517

518

519

520 **Fig. 5 –** SEM images of pure ARM (Top left), and SD systems respectively F3 (A&B), F6

521 (C), F9 (D), F12 (E).

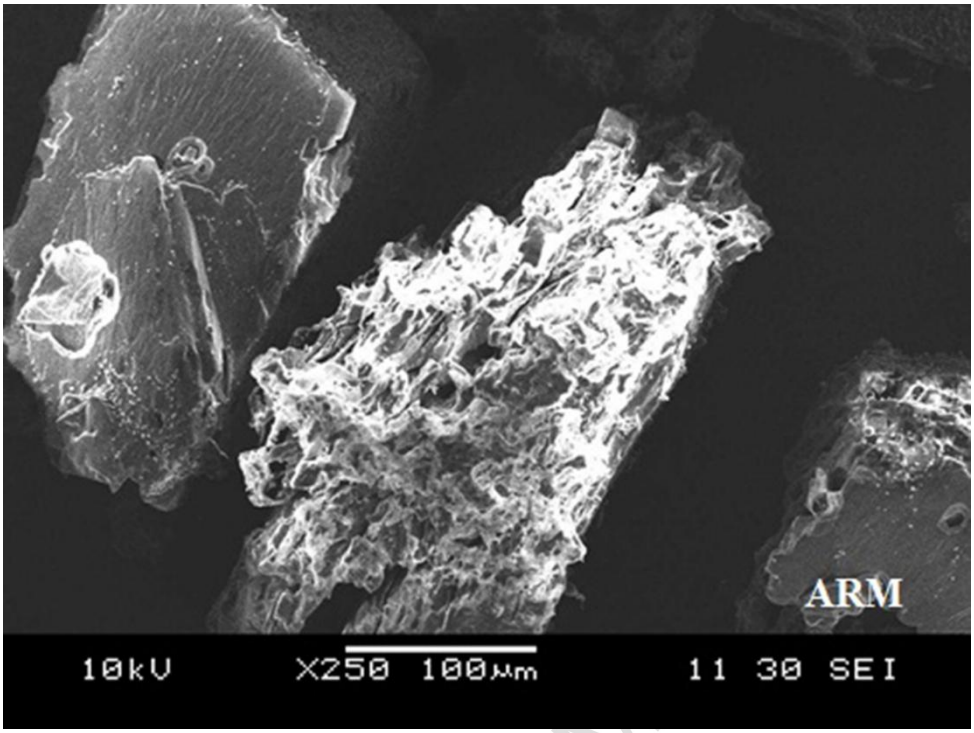

522

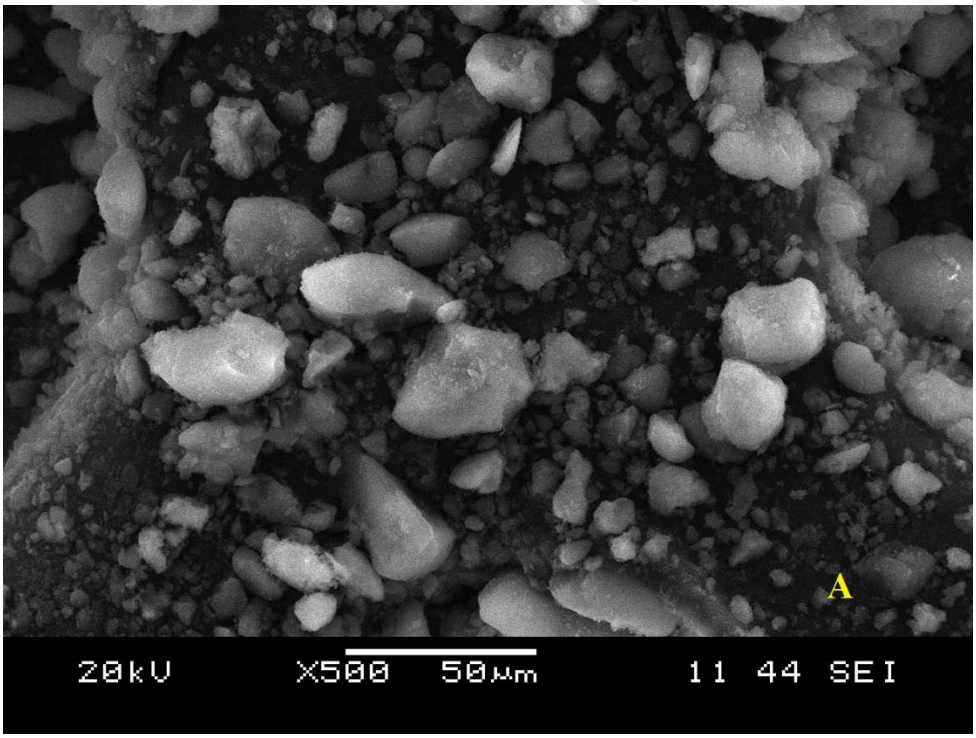

523

524

525

526

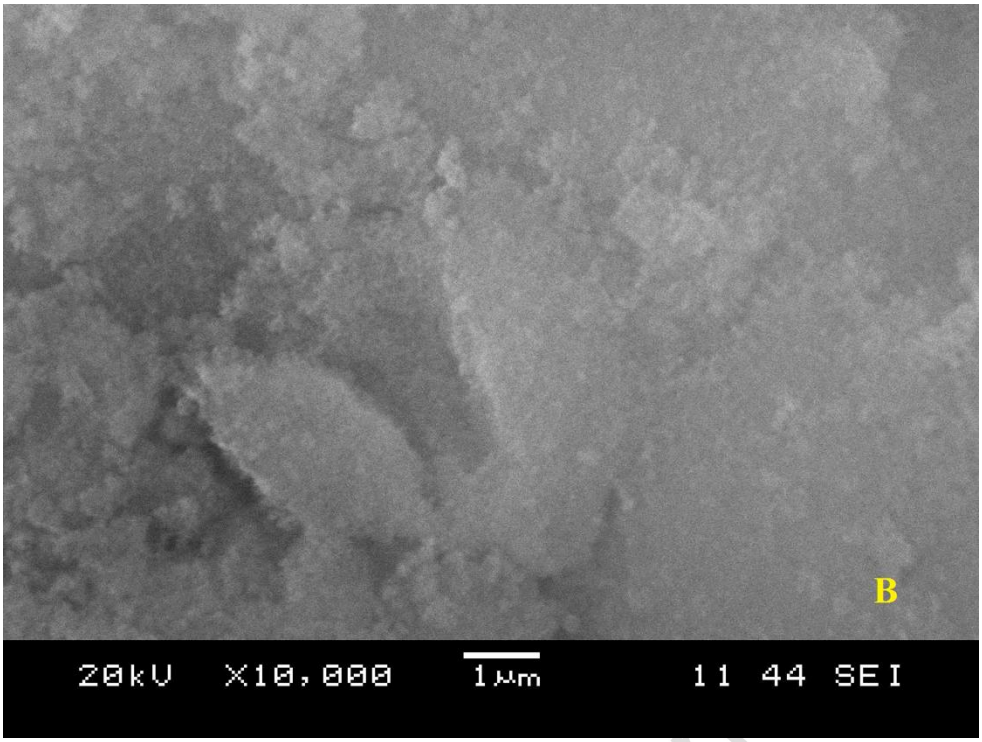

527

528

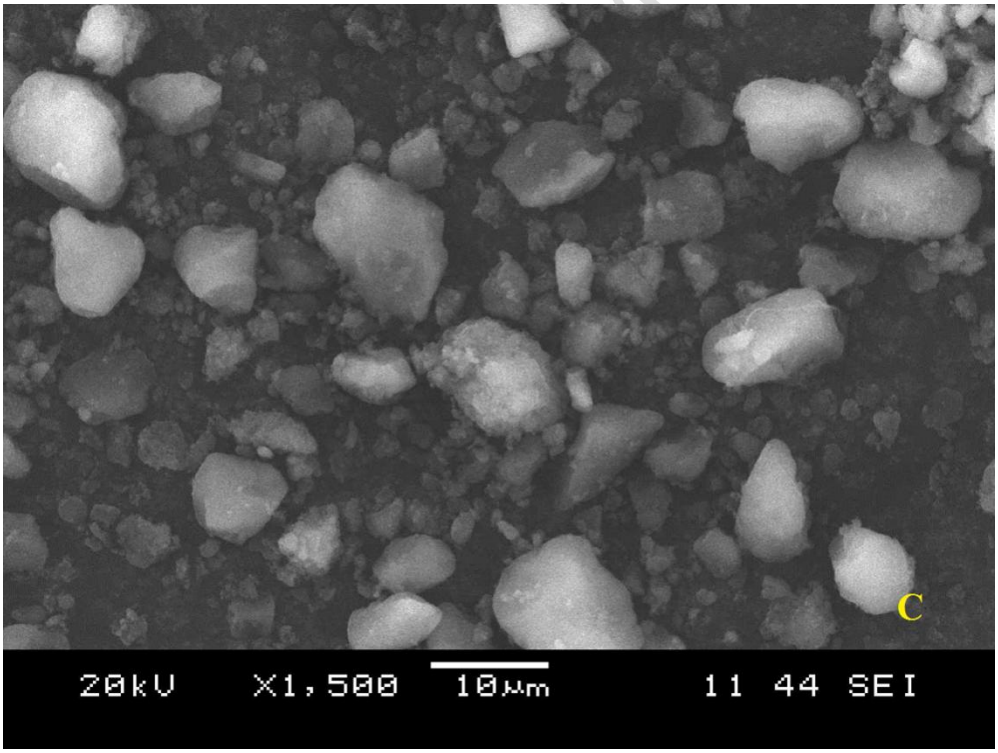

529

530

531

532

533

534

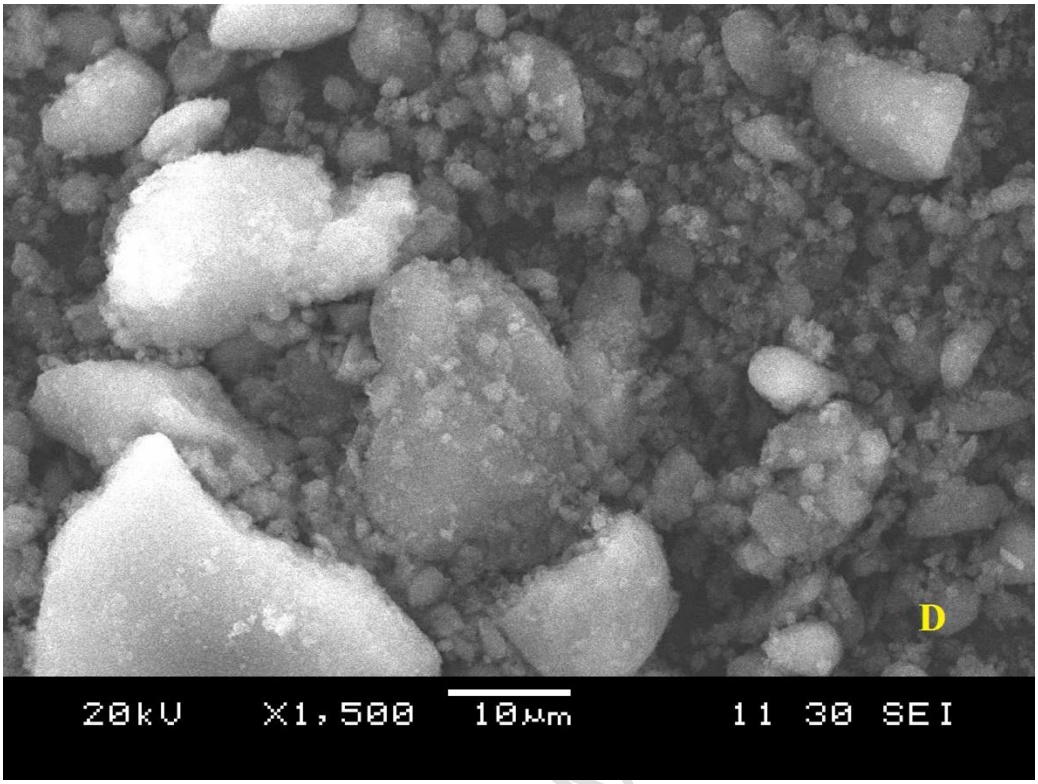

535

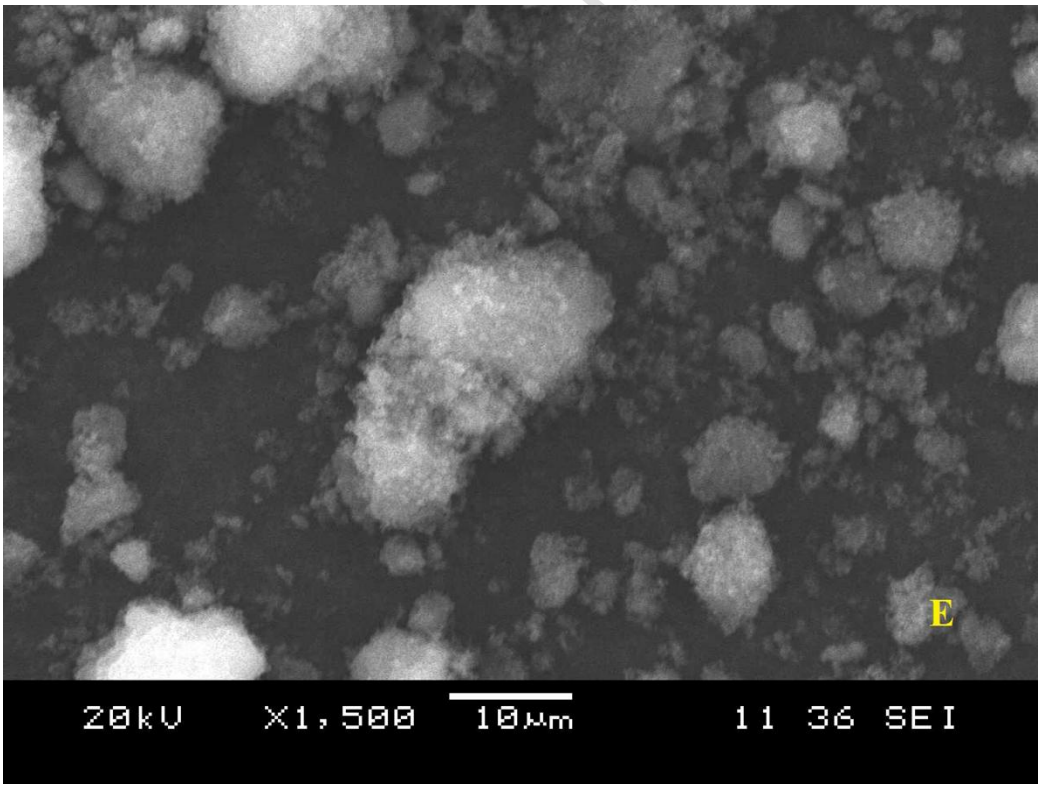

536

537

538

Fig. 6. *In vitro* release of ARM SD formulation batches in phosphate buffer pH 7.2 containing 1% SLS (mean ± SD)

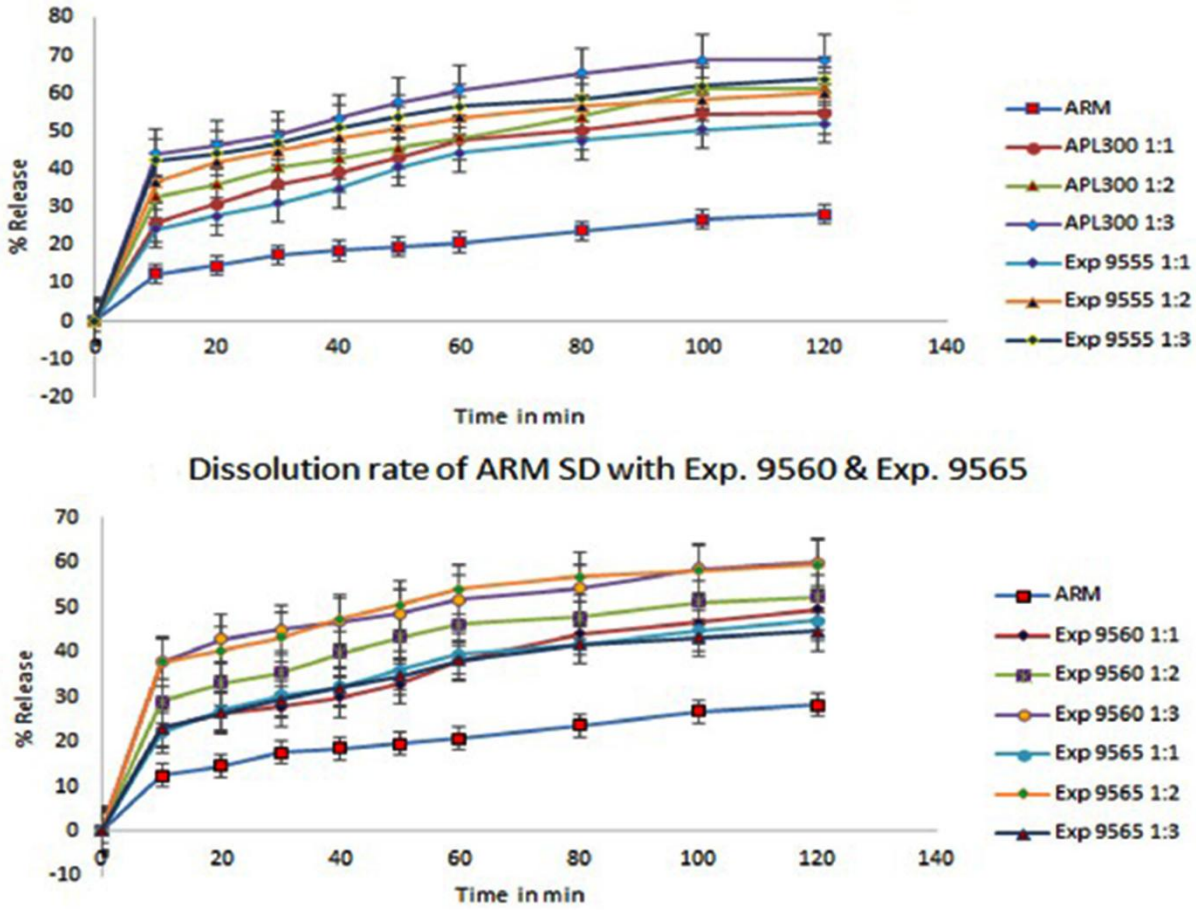

548 **Fig. 7.** Nitrogen adsorption-desorption isotherms of the porous silica samples; (A) APL 300

549 (B) Exp. 9555, (C) Exp. 9560, (D) Exp. 9565.

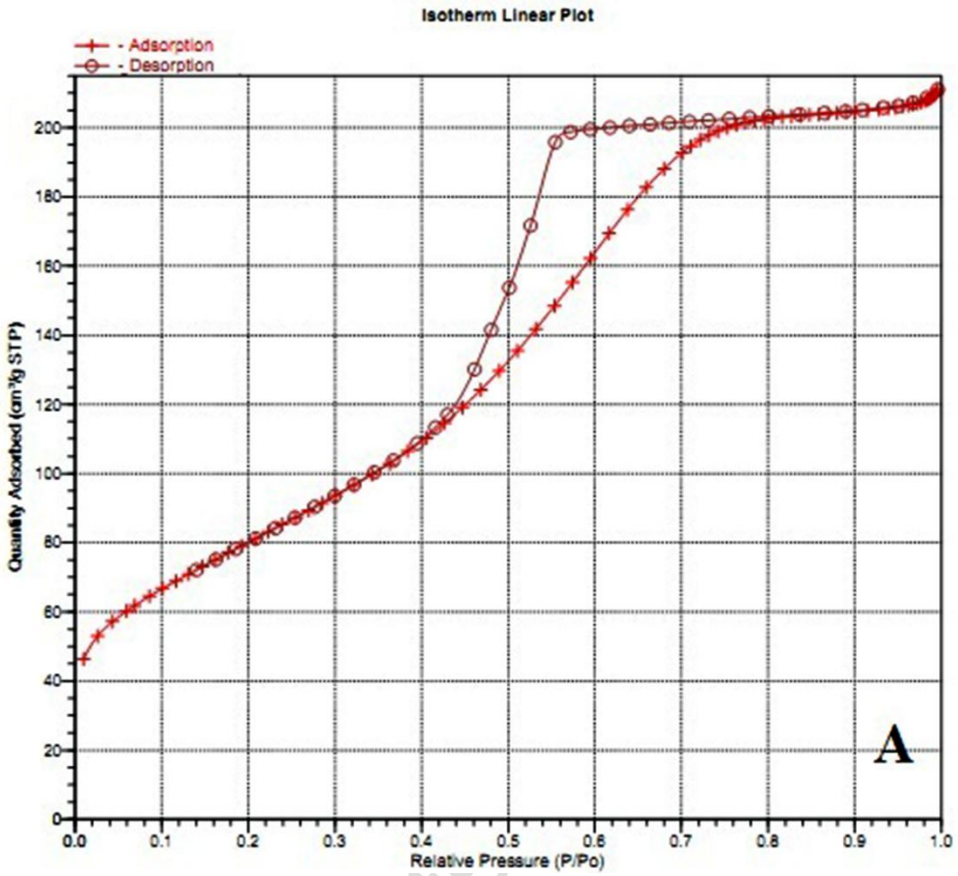

550

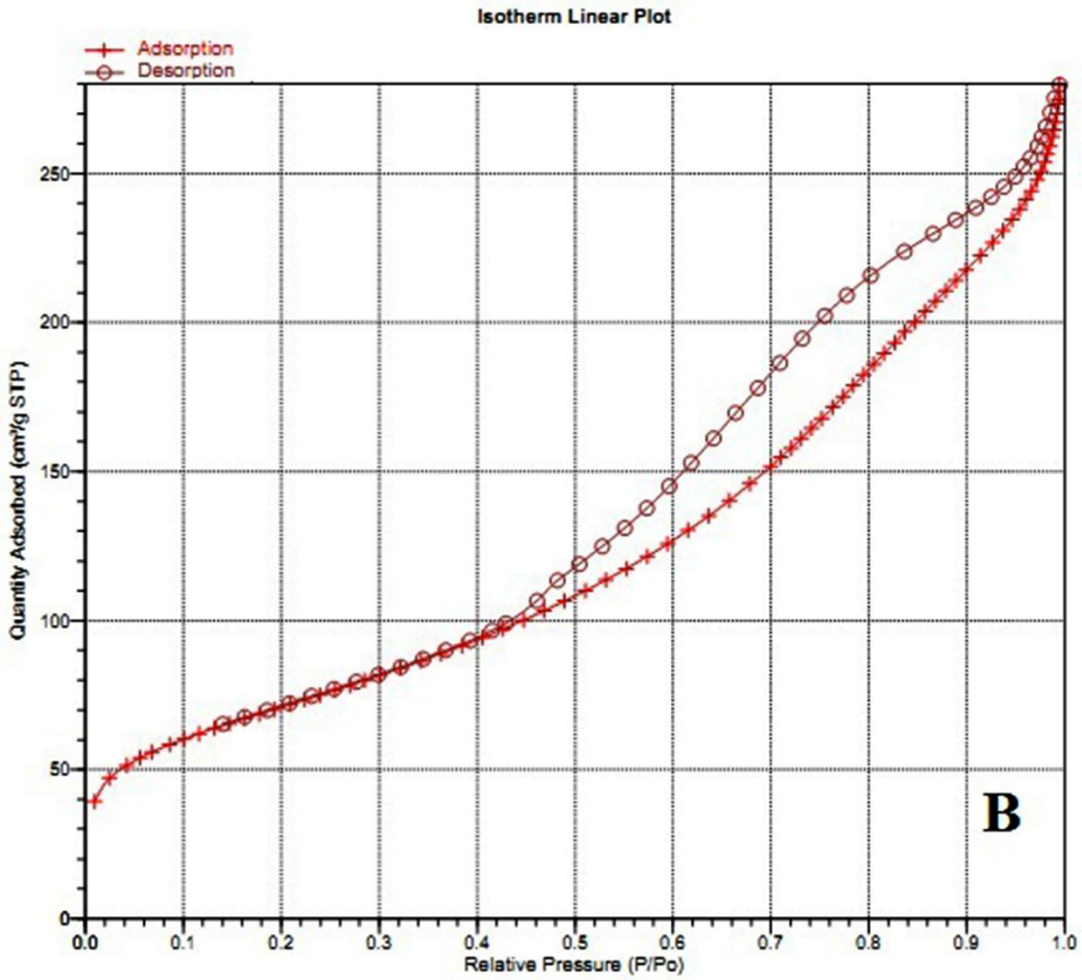

551

552

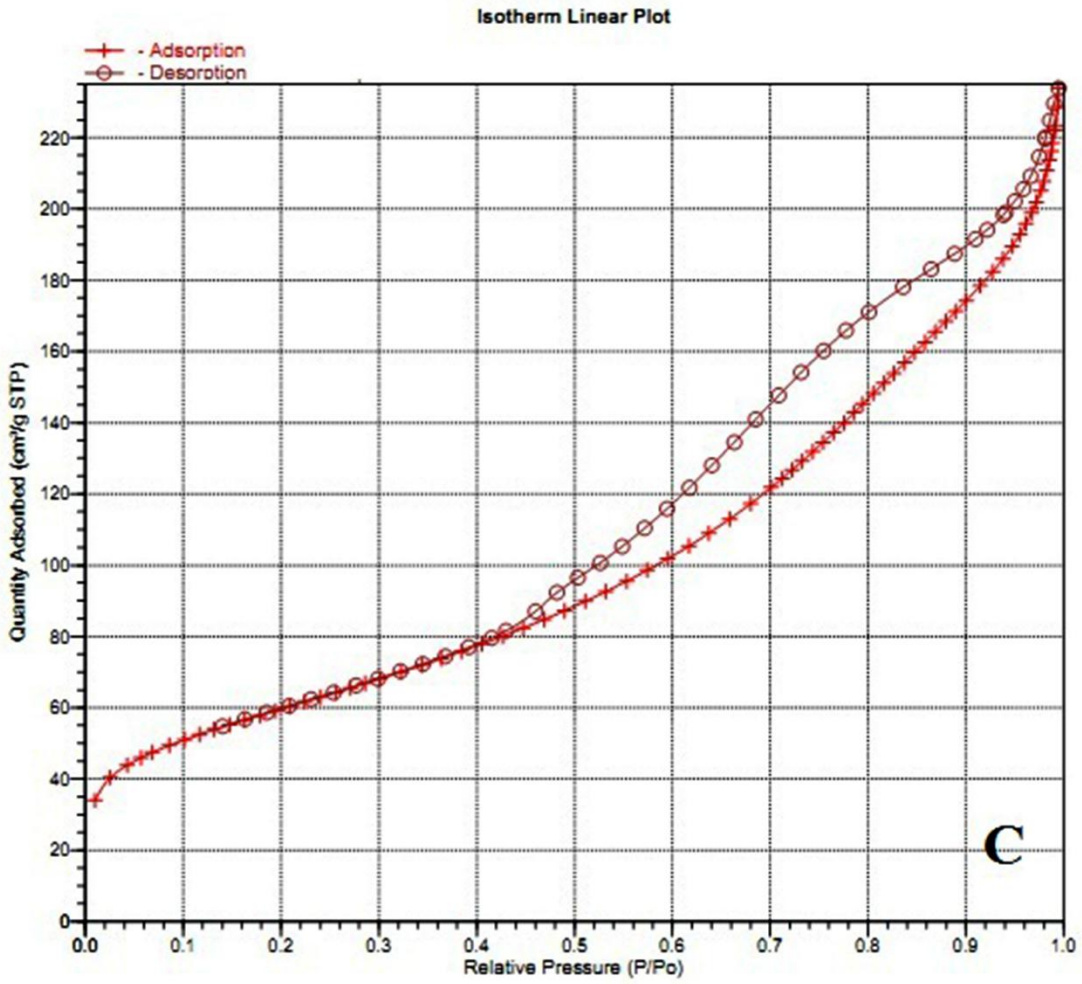

553

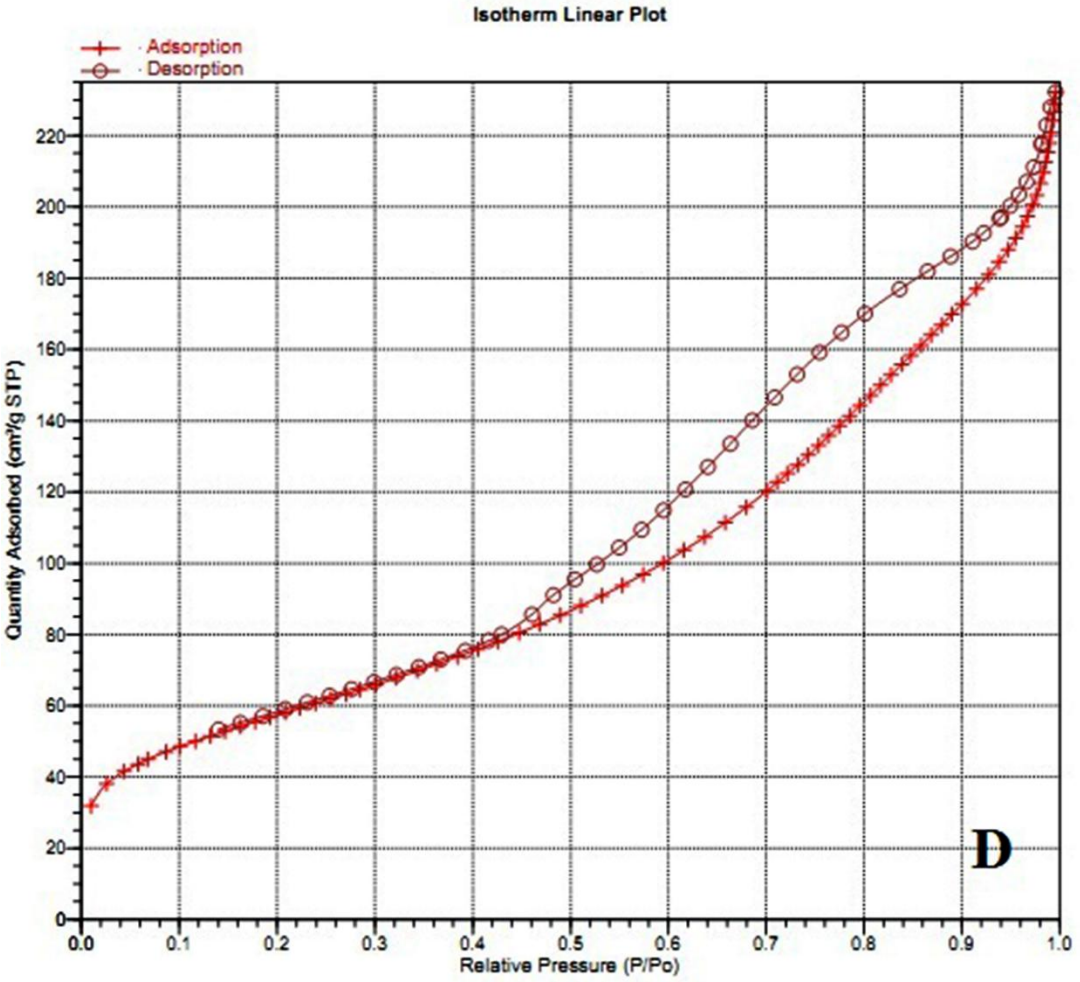

554

555

556

557

558 **Table 1.** Composition of ARM:PS systems

Batch code	Formulation batch composition	% Ratio	Batch size (gm)
F1	ARM: APL300	1:1	10
F2	ARM: APL300	1:2	15
F3	ARM: APL300	1:3	20
F4	ARM: EXP.9555	1:1	10
F5	ARM: EXP.9555	1:2	15
F6	ARM: EXP.9555	1:3	20
F7	ARM: EXP.9560	1:1	10
F8	ARM: EXP.9560	1:2	15

F9	ARM: EXP.9560	1:3	20
F10	ARM: EXP.9565	1:1	10
F11	ARM: EXP.9565	1:2	15
F12	ARM: EXP.9565	1:3	20

559

560 **Table 2**. Micrometrics properties of ARM:PS systems

Parameters	ARM: APL 300	ARM:EXP.9555	ARM:EXP.9560	ARM:EXP.9565
Bulk density (gm/ml)	0.223±0.003	0.222±0.006	0.299±0.003	0.222±0.006

Tapped density (gm/ml)	0.279±0.010	0.285±0.013	0.341±0.007	0.285±0.011
Hausner's ratio	1.24±0.009	1.28±0.015	1.31±0.003	1.28±0.012
Carr's Index	19.78±0.014	22.1±0.008	24.28±0.03	22.1±0.011
Angle of repose	24.35°±0.962	25.43°±1.01	29.35°±1.24	28.34°±1.13

561

562 **Table 3**. Moisture content of all ARM:PS systems

% Moisture content	ARM: APL 300	ARM: EXP.9555	ARM: EXP.9560	ARM: EXP.9565

1:1	6.612	9.015	5.435	6.667
1:2	6.602	9.019	5.445	6.670
1:3	6.622	9.033	5.450	6.660

563

564 **Table 4.** Content uniformity of optimized ARM:PS systems

% ARM Content uniformity	ARM: APL 300	ARM: EXP.9555	ARM: EXP.9560	ARM:EXP.9565
1:1	100.88	101.57	100.74	101.29
1:2	97.71	99.91	98.95	97.99
1:3	99.91	97.30	97.99	98.54

565

566